SUPPLEMENTAL MATERIALS

Mechano-covalent protection of coagulation factor VIII by von Willebrand factor

Diego Butera, Haoqing Jerry Wang, Heng-Giap Woon, Yunduo Charles Zhao, Lining Arnold Ju, Philip J. Hogg

Table S1. **VWF cysteine containing peptides analysed by HPLC and mass spectrometry**. Cysteine numbering is according to UniProt identifier P02671 for human VWF. The Cys residues of the disulfide that were measured are underlined in the peptide.

Cys measured	Disulfide bond	Peptide
767	767-808	SLSCRPPMVK
776	776-804	LVCPADNLR
788	788-799	AEGLECTK
821	810-821	CVALER
827	792-827	CPCFHQGK
829	829-851	CPCFHQGK
914	914-921	GCSHPSVK
1031	889-1031	VSSQCADTR
1046	1046-1089	KVPLDSSPATCHNNIMK
1060	1060-1084	QTMVDSSCR
1071	1071-1111	ILTSDVFQDCNK
1126	1101-1126	TATLCPQSCEER
1130	1130-1173	TATLCPQSCEER

Table S2. **HPLC retention times of VWF peptides and ^{12}C-IPA- and ^{13}C-IPA-labelled peptide peak areas for the 13 healthy donor proteins**. Values for peptides containing a single Cys are listed. For peptides containing two Cys (CPCFHQGK and TATLCPQSCEER) we obtain 3 populations: one where both Cys are labelled with ^{12}C-IPA, one where both Cys are labeled with ^{13}C-IPA, and a mixed population where one Cys is labelled with ^{12}C-IPA and the other with ^{13}C-IPA at either position. The mixed populations have the same retention time and mass. To distinguish between them, we select fragments from MS2 that have unique mass signatures for one or the other. Since each mass has intensity values we compare the total intensities for both peptides and find their ratio.

Sample	Cysteine	Peptide	Retention time, min	^{12}C-IPA peak area	^{13}C-IPA peak area	Fraction Unformed
Healthy donor 1	767	SLSCRPPMVK	33.33	116236	1534420	0.07
	776	LVCPADNLR	37.55	2040829	13835218	0.129
	788	AEGLECTK	31.06	212652	3920495	0.051
	821	CVALER	33.54	248974	4834228	0.049
	914	GCSHPSVK	25.99	197480	2886057	0.064
	1031	VSSQCADTR	27.12	419503	9221315	0.044
	1046	KVPLDSSPATCHNNIMK	32.18	319294	3042286	0.095
	1060	QTMVDSSCR	30.53	234096	2959111	0.073
	1071	ILTSDVFQDCNK	38.21	402641	19749232	0.02
Healthy donor 2	767	SLSCRPPMVK	33.41	87688	1314023	0.063
	776	LVCPADNLR	37.65	1779112	10446320	0.146
	788	AEGLECTK	31.13	209105	3014212	0.065
	821	CVALER	33.66	362001	6249348	0.055

	914	GCSHPSVK	25.98	332702	2277522	0.127
	1031	VSSQCADTR	27.10	407707	7771284	0.05
	1046	KVPLDSSPATCHNNIMK	32.30	340158	2846348	0.107
	1060	QTMVDSSCR	30.61	263579	2391221	0.099
	1071	ILTSDVFQDCNK	38.27	361947	14589928	0.024
Healthy donor 3	767	SLSCRPPMVK	33.46	163157	1250788	0.115
	776	LVCPADNLR	37.73	1882305	8837055	0.176
	788	AEGLECTK	31.17	389462	5687065	0.064
	821	CVALER	33.67	379432	4590300	0.076
	914	GCSHPSVK	26.02	197517	2126561	0.085
	1031	VSSQCADTR	27.10	369175	7456970	0.047
	1046	KVPLDSSPATCHNNIMK	32.34	288945	2142992	0.119
	1060	QTMVDSSCR	30.64	259043	2285694	0.102
	1071	ILTSDVFQDCNK	38.35	310969	12097733	0.025
Healthy donor 4	767	SLSCRPPMVK	33.36	340360	2221409	0.133
	776	LVCPADNLR	37.63	3068815	13526880	0.185
	788	AEGLECTK	31.08	698928	9073087	0.072
	821	CVALER	33.57	597456	5754159	0.094
	914	GCSHPSVK	25.98	396112	3661863	0.098
	1031	VSSQCADTR	27.08	910226	13906553	0.061
	1046	KVPLDSSPATCHNNIMK	32.23	653451	4106989	0.137
	1060	QTMVDSSCR	30.54	629859	4178620	0.131
	1071	ILTSDVFQDCNK	38.29	635590	18440844	0.033
Healthy donor 5	767	SLSCRPPMVK	33.28	86550	992951	0.08
	776	LVCPADNLR	37.54	1525524	9598812	0.137
	788	AEGLECTK	31.00	382411	6114311	0.059
	821	CVALER	33.50	254038	4532524	0.053
	914	GCSHPSVK	25.87	229000	2530689	0.083
	1031	VSSQCADTR	26.99	514481	10243747	0.048
	1046	KVPLDSSPATCHNNIMK	32.15	375210	2183902	0.147
	1060	QTMVDSSCR	30.47	223868	2222509	0.092
	1071	ILTSDVFQDCNK	38.20	320643	14173705	0.022
Healthy donor 6	767	SLSCRPPMVK	33.27	103101	669516	0.133
	776	LVCPADNLR	37.56	1776205	8720259	0.169
	788	AEGLECTK	31.00	206338	2181213	0.086
	821	CVALER	33.50	287556	3411665	0.078
	914	GCSHPSVK	25.86	199123	1691560	0.105
	1031	VSSQCADTR	27.02	443194	5845594	0.07
	1046	KVPLDSSPATCHNNIMK	32.11	374735	1898119	0.165
	1060	QTMVDSSCR	30.50	278788	1632459	0.146
	1071	ILTSDVFQDCNK	38.20	501475	12768986	0.038
Healthy donor 7	767	SLSCRPPMVK	33.38	248051	1799805	0.121
	776	LVCPADNLR	37.63	2504011	12692088	0.165
	788	AEGLECTK	31.11	240955	3906892	0.058
	821	CVALER	33.60	510914	5930250	0.079
	914	GCSHPSVK	26.02	359316	3019603	0.106
	1031	VSSQCADTR	27.15	626932	11016803	0.054
	1046	KVPLDSSPATCHNNIMK	32.22	660170	3534738	0.157
	1060	QTMVDSSCR	30.57	435995	3261724	0.118
	1071	ILTSDVFQDCNK	38.29	491858	17129106	0.028
	767	SLSCRPPMVK	33.27	270275	1859076	0.127
	776	LVCPADNLR	37.54	4121855	19927312	0.171

Healthy donor 8	788	AEGLECTK	31.02	350873	5202326	0.063
	821	CVALER	33.49	706614	7830872	0.083
	914	GCSHPSVK	25.96	479798	4187845	0.103
	1031	VSSQCADTR	27.08	837375	16465369	0.048
	1046	KVPLDSSPATCHNNIMK	32.13	713149	4905737	0.127
	1060	QTMVDSSCR	30.52	582551	4117727	0.124
	1071	ILTSDVFQDCNK	38.18	1021248	26197340	0.038
Healthy donor 9	767	SLSCRPPMVK	34.56	158074	502964	0.239
	776	LVCPADNLR	39.27	3335133	8718460	0.277
	788	AEGLECTK	32.02	701928	5540963	0.112
	821	CVALER	34.79	652926	3662864	0.151
	914	GCSHPSVK	26.35	171624	949592	0.153
	1031	VSSQCADTR	27.70	740645	8487754	0.08
	1046	KVPLDSSPATCHNNIMK	33.21	455936	884235	0.34
	1060	QTMVDSSCR	31.44	862301	1909894	0.311
	1071	ILTSDVFQDCNK	39.89	544344	10659590	0.049
Healthy donor 10	767	SLSCRPPMVK	35.07	347230	1075439	0.244
	776	LVCPADNLR	39.78	2991781	7205544	0.293
	788	AEGLECTK	32.37	316689	2297864	0.121
	821	CVALER	35.21	501484	2295740	0.179
	914	GCSHPSVK	26.66	171097	739990	0.188
	1031	VSSQCADTR	27.95	921549	7997055	0.103
	1046	KVPLDSSPATCHNNIMK	33.60	638129	1567329	0.289
	1060	QTMVDSSCR	31.76	1081924	3655520	0.228
	1071	ILTSDVFQDCNK	40.33	470047	9312739	0.048
Healthy donor 11	767	SLSCRPPMVK	32.59	1652473	4966335	0.25
	776	LVCPADNLR	36.63	11078342	25962422	0.299
	788	AEGLECTK	30.31	3270600	21728042	0.131
	821	CVALER	32.82	1798057	9257014	0.163
	914	GCSHPSVK	25.35	1742347	8162783	0.176
	1031	VSSQCADTR	26.61	3703688	31681901	0.105
	1046	KVPLDSSPATCHNNIMK	31.41	3027972	11170003	0.213
	1060	QTMVDSSCR	29.80	1491445	6409002	0.189
	1071	ILTSDVFQDCNK	37.14	3037437	37695245	0.075
Healthy donor 12	767	SLSCRPPMVK	32.49	1072188	3234180	0.249
	776	LVCPADNLR	36.55	18281243	51537181	0.262
	788	AEGLECTK	30.29	2592471	20076684	0.114
	821	CVALER	32.82	1694643	11337080	0.13
	914	GCSHPSVK	25.36	2317614	12194651	0.16
	1031	VSSQCADTR	26.67	7395620	54170284	0.12
	1046	KVPLDSSPATCHNNIMK	31.32	3885421	15457825	0.201
	1060	QTMVDSSCR	29.76	3227551	16938862	0.16
	1071	ILTSDVFQDCNK	37.12	3998533	50396829	0.074
Healthy donor 13	767	SLSCRPPMVK	32.39	6335334	19520274	0.245
	776	LVCPADNLR	36.61	25853353	52732538	0.329
	788	AEGLECTK	30.14	5593052	30492252	0.155
	821	CVALER	32.69	3061169	11740347	0.207
	914	GCSHPSVK	25.32	3116553	12474461	0.2
	1031	VSSQCADTR	26.65	8921426	61649772	0.126
	1046	KVPLDSSPATCHNNIMK	31.27	9342262	29465783	0.241
	1060	QTMVDSSCR	29.71	3668353	14521872	0.202
	1071	ILTSDVFQDCNK	37.18	5570691	54260478	0.093

Table S3. **Redox states of the 7 male and 6 female VWF TIL'-TIL3 domain disulfide bonds**. Mean and SD and coefficient of variation is listed. Graphical representation of the experimental data shown in Fig. 1C.

Disulfide bond	Male (n=7) mean fraction unformed ± SD	Male (n=7) Coeff. of variation	Female (n=6) mean fraction unformed ± SD	Female (n=6) Coeff. of variation
767-808	0.176 ± 0.065	37.0%	0.139 ± 0.085	61.3%
776-804	0.224 ± 0.069	31.0%	0.195 ± 0.075	38.2%
788-799	0.095 ± 0.037	38.7%	0.082 ± 0.032	39.4%
792-827	0.102 ± 0.049	48.6%	0.097 ± 0.061	63.0%
810-821	0.119 ± 0.055	45.9%	0.094 ± 0.051	54.7%
829-851	0.073 ± 0.039	53.6%	0.068 ± 0.036	52.5%
889-1031	0.081 ± 0.035	42.4%	0.065 ± 0.024	36.7%
914-921	0.135 ± 0.046	34.2%	0.117 ± 0.043	36.8%
1046-1089	0.186 ± 0.062	33.5%	0.173 ± 0.092	52.9%
1060-1084	0.154 ± 0.046	30.0%	0.149 ± 0.089	59.7%
1071-1111	0.049 ± 0.025	51.5%	0.037 ± 0.021	56.9%
1101-1126	0.079 ± 0.063	80.3%	0.074 ± 0.029	39.6%
1130-1173	0.115 ± 0.040	34.9%	0.077 ± 0.046	59.6%

Table S4. **Redox states of 3 healthy donor plasma VWF TIL'-TIL3 domain disulfide bonds (2 males, 1 female) when unbound or bound to FVIII**. Statistics of the results shown in Fig. 3A. Discovery determined using the two-stage linear step-up procedure of Benjamini, Krieger and Yekutieli, with Q = 1%. Each row was analyzed individually, without assuming a consistent SD.

Disulfide bond	VWF mean fraction unformed	VWF·FVIII mean fraction unformed	Difference ± SE	P value
767-808	0.2529	0.1204	0.133 ± 0.010	0.000189
776-804	0.2964	0.2017	0.095 ± 0.016	0.004405
788-799	0.1465	0.07661	0.070 ± 0.008	0.000739
792-827	0.1300	0.08862	0.041 ± 0.029	0.222709
810-821	0.1692	0.07543	0.094 ± 0.022	0.013360
829-851	0.09293	0.03808	0.055 ± 0.018	0.036858
889-1031	0.1367	0.09197	0.045 ± 0.003	0.000131
914-921	0.1769	0.1186	0.058 ± 0.006	0.000535
1046-1089	0.2590	0.1601	0.099 ± 0.008	0.000279
1060-1084	0.2206	0.1048	0.116 ± 0.003	0.000002
1071-1111	0.08600	0.03818	0.048 ± 0.003	0.000044
1101-1126	0.09177	0.04906	0.043 ± 0.005	0.000997
1130-1173	0.2041	0.1348	0.069 ± 0.011	0.003519

Table S5. **Heart failure (HF) and ECMO patient VWF and FVIII characteristics**. Normal ranges are indicated in brackets.

Patient	**Factor VIII, %** (50-150)	**VWF Antigen, IU/dL** (50-200)	**VWF RCo, %** (50-150)	**VWF CBA, IU/dL** (50-200)	**VWF RCo/Antigen**	**VWF CBA/Antigen**	**Ultra-large VWF**
HF1	277	246	167	171	0.678862	0.695122	Normal
HF2	324	315	202	172	0.64127	0.546032	N/A
HF3	192	164	99	107	0.603659	0.652439	Normal
HF4	133	162	94	131	0.580247	0.808642	Normal
HF5	229	332	221	189	0.665663	0.569277	Normal
ECMO1	308	510	226	202	0.443137	0.396078	Loss
ECMO2	594	513	184	155	0.358674	0.302144	Loss
ECMO3	316	345	219	144	0.634783	0.417391	Loss
ECMO4	507	592	390	155	0.658784	0.261824	Loss
ECMO5	383	434	346	164	0.797235	0.377880	Loss

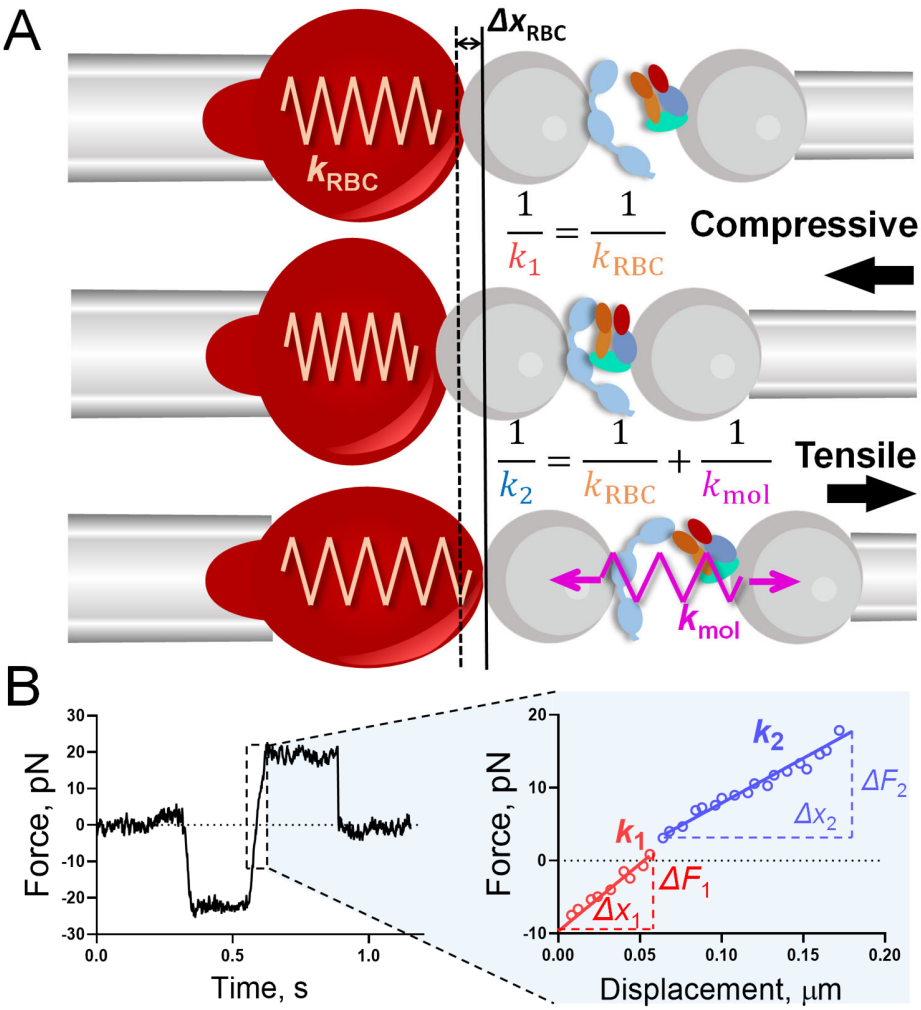

Figure S1. Calculation of molecular spring constant, k_{mol}, for BFP assay. **A**. Schematic of a BFP touch cycle. Based on Hooke's law, the compressive and tensile forces can be quantified by the product of the spring constant and displacement of the probe bead Δx_{RBC}. Notably, the molecular bond is not stretched during the compressive state, therefore k_{mol} is not considered. **B**. Deriving k_{mol} by converting Force *vs*. Time curve to Force *vs*. Displacement curve. *Left:* Representative force spectroscopy of a BFP bond touch cycle. *Right:* converted Force vs. Displacement curve during the retraction of the BFP cycle. Least-squares linear regression was employed to obtain k_1 (*red line*) and k_2 (*blue line*), respectively. The total spring constant during the compressvie state (k_1) is displayed as:

$$\frac{1}{k_1} = \frac{1}{k_{RBC}} \quad (1)$$

At the tensile stage, the total spring constant would remain as k_1 until the molecular bond was formed and stretched. As a result, the spring constant at the tensile stage (k_2) is represented as:

$$\frac{1}{k_2} = \frac{1}{k_{RBC}} + \frac{1}{k_{mol}} \quad (2)$$

To derive k_{mol}, the force spectroscopy of each bond event during retraction was converted into a Force *vs*. Displacement curve by multiplying the time by the actuation speed of the Target (i.e., 4,000 nm/s) [1].

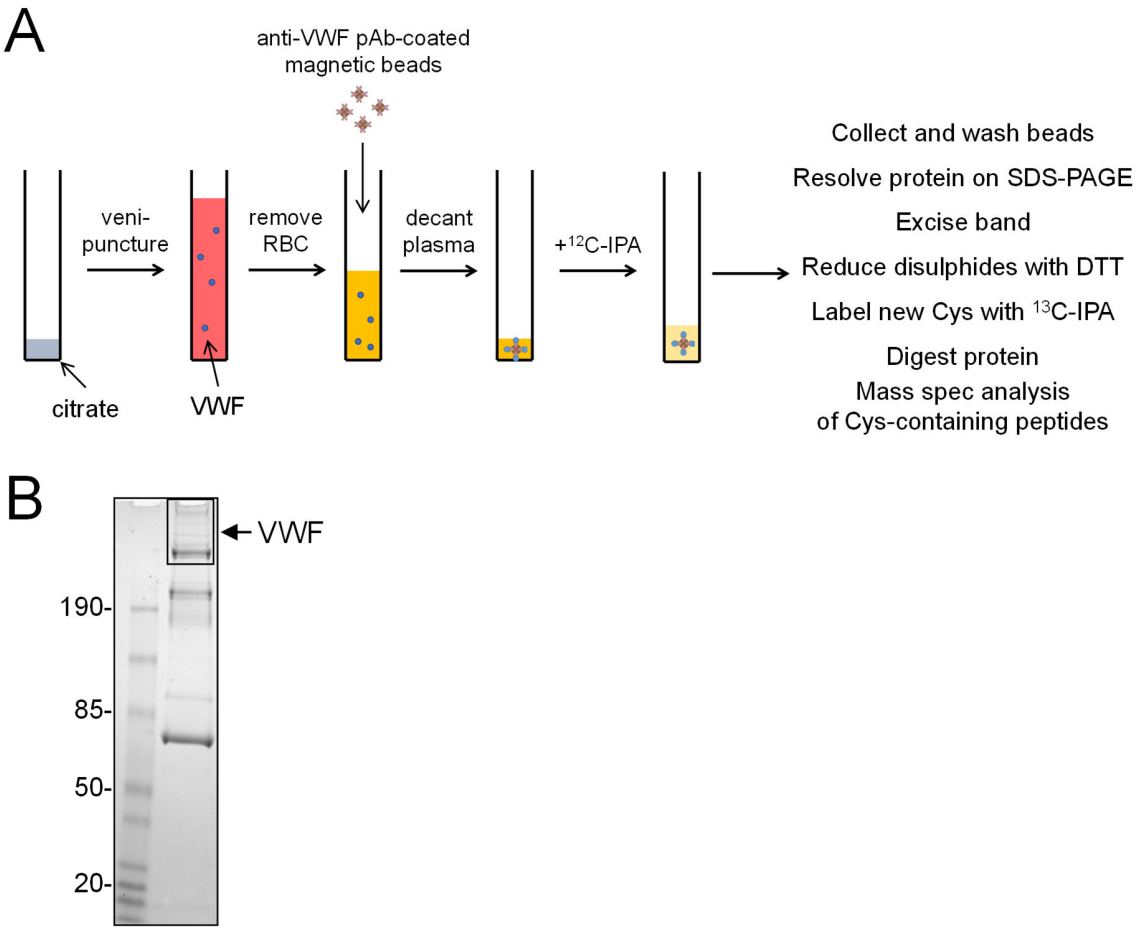

Figure S2. **Methods for measuring the redox state of VWF disulfide bonds**. **A**. Blood from healthy donors was drawn by venipuncture into citrate as anti-coagulant, plasma prepared by centrifugation and VWF collected on antibody-coated magnetic beads. The unpaired cysteine thiols in bead-bound VWF were alkylated with ^{12}C-IPA, the protein resolved on SDS-PAGE and the disulfide-bonded cysteine thiols alkylated with ^{13}C-IPA following reduction with DTT. The protein was digested with trypsin, 13 peptides (Table S1) encompassing cysteines representing 6 of the 8 disulfide bonds in the VWF TIL' and E' domains and 7 of the 14 disulfide bonds in the D3 through TIL3 domains were analyzed by HPLC and mass spectrometry and the redox state of the disulfides quantified. **B**. Example of ^{12}C-IPA-labelled VWF resolved on SDS-PAGE. All multimer forms of VWF were excised from the gel (indicated by the box) and processed for disulfide bond redox state. For reference, the VWF dimer has a molecular mass of 500 kDa. Molecular mass standards are shown in the left-hand lane.

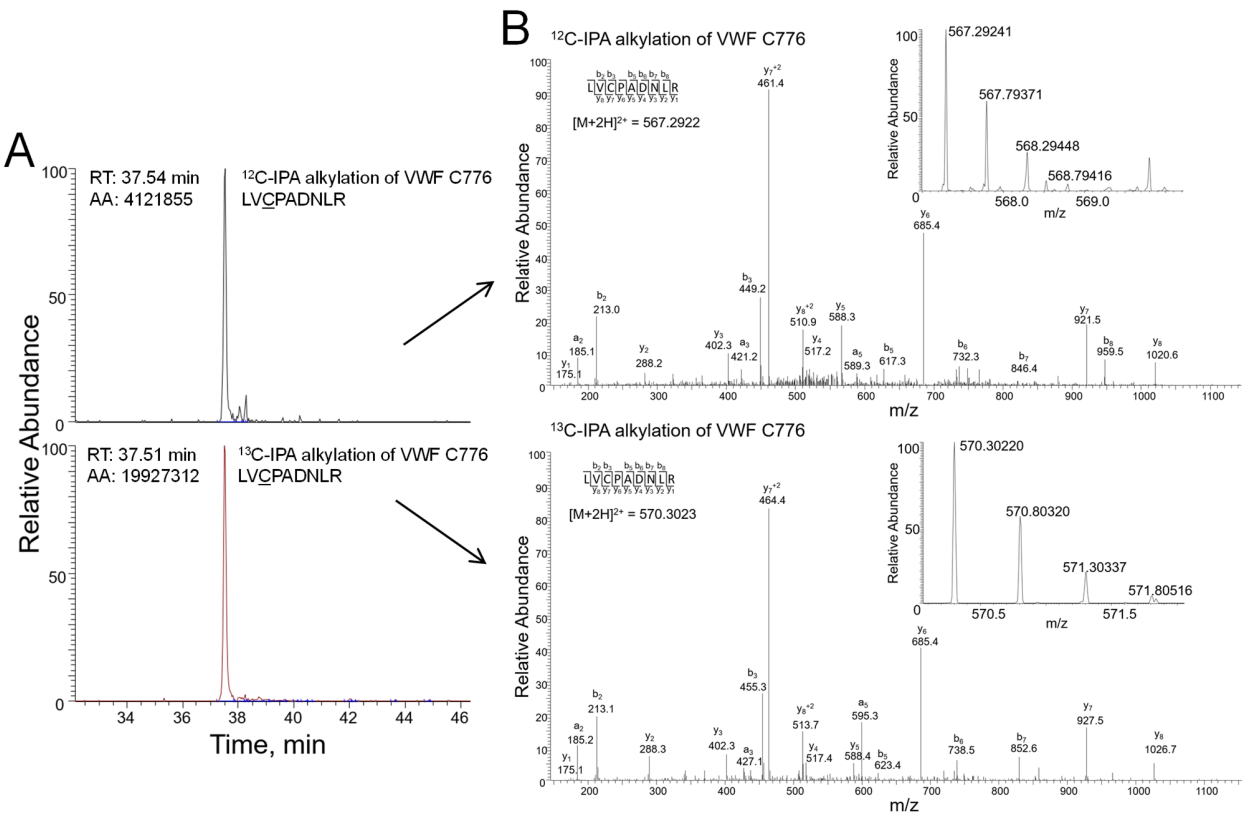

Figure S3. **Differential cysteine alkylation of the VWF C776 residue and peptide analysis**. **A**. HPLC resolution of the LVCPADNLR peptide containing C776 labelled with either ^{12}C-IPA (upper trace) or ^{13}C-IPA (lower trace). **B**. Representative tandem mass spectra of the LVCPADNLR peptide. The upper and lower traces are examples of ^{12}C-IPA or ^{13}C-IPA alkylation of C776, respectively. The accurate mass spectrum of the peptide is shown in the insets (upper trace, observed $[M+2H]^{2+}$ = 567.2924 m/z and expected $[M+2H]^{2+}$ = 567.2922 m/z; lower trace, observed $[M+2H]^{3+}$ = 570.3022 m/z and expected $[M+2H]^{2+}$ = 570.3023).

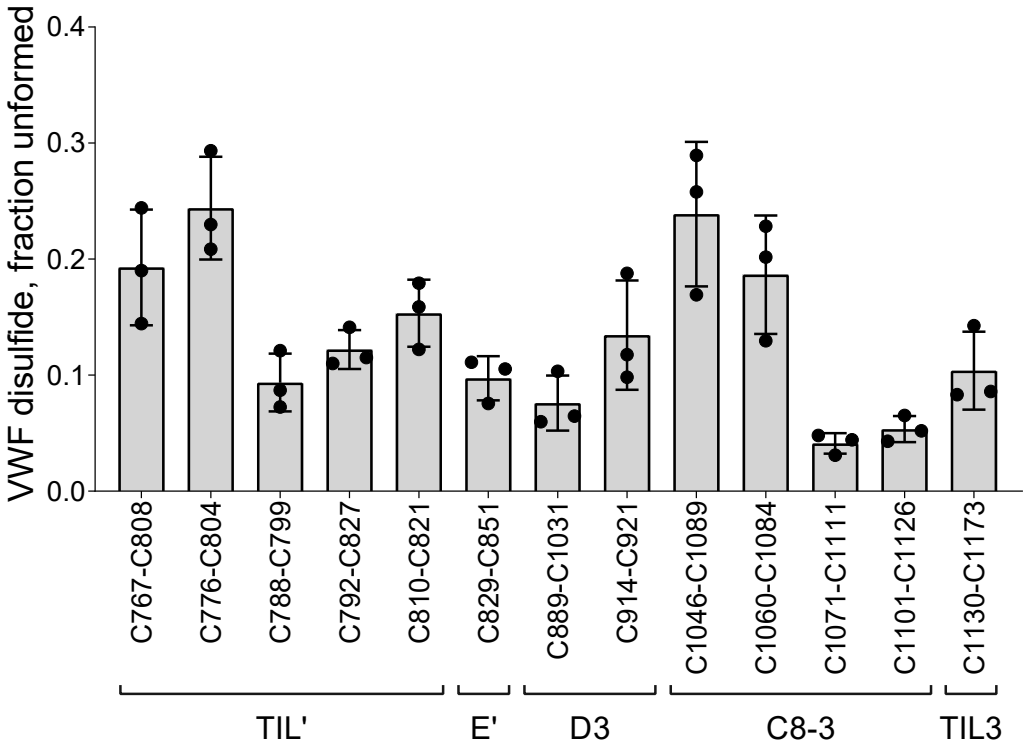

Figure S4. Inter-assay variation in redox states of the VWF TIL'-TIL3 domain disulfide bonds. A single plasma sample (32 year old male) was assayed on three separate occasions. The average coefficient of variation for the 13 disulfides was 26.4%.

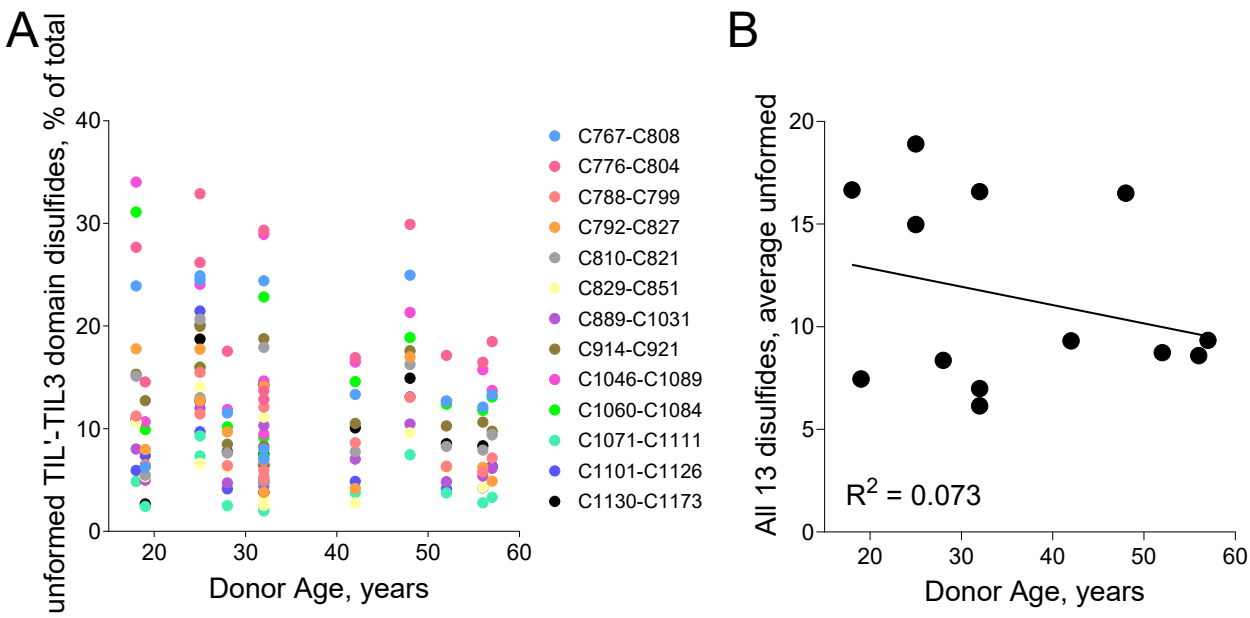

Figure S5. Age dependence in redox states of the VWF TIL'-TIL3 domain disulfide bonds. **A**. Redox states of the 13 TIL-TIL3 disulfides in 13 healthy human donors expressed as a function of donor age (18-57 years old). **B**. Correlation of average redox state of the 13 disulfides as a function of donor age. The solid line is the linear least-squares fit of the data, which is not significantly non-zero.

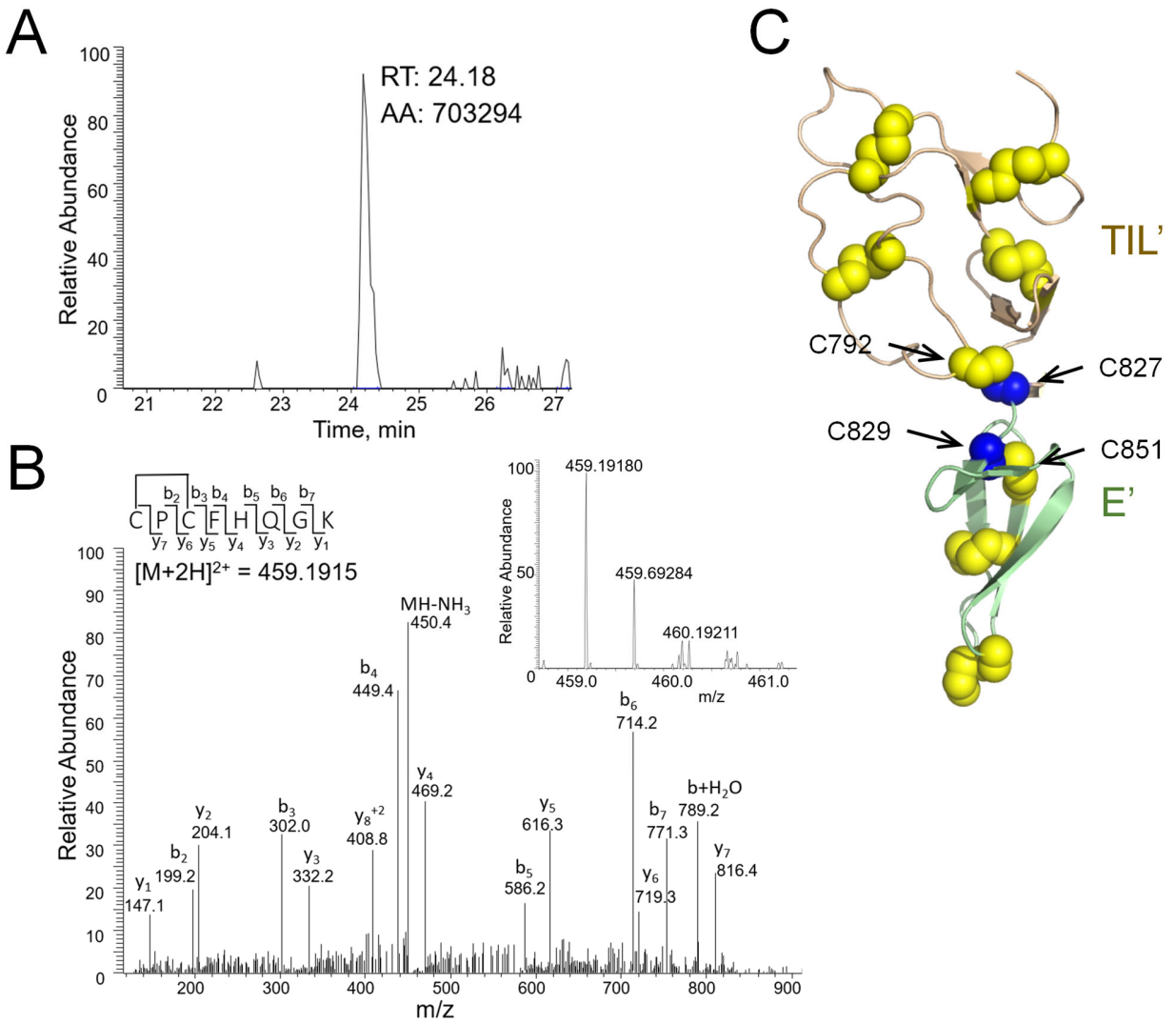

Figure S6. **Identification of the VWF C827-C829 disulfide bond**. **A**. HPLC resolution of the CPCFHQGK peptide containing C827 in the TIL' domain linking C829 in the E' domain in VWF from healthy donor plasma. **B**. Representative tandem mass spectra of the CPCFHQGK peptide. The accurate mass spectrum of the peptide is shown in the inset (observed $[M+2H]^{2+}$ = 459.1918 m/z and expected $[M+2H]^{2+}$ = 459.1915 m/z). **C**. Ribbon representation of the crystal structure of the TIL' (residues 764-827 in wheat) and E' (residues 828-863 in light green) domains of VWF [2] (PDB identifier 6n29). Cysteines are shown as yellow or blue spheres. C792, C827, C829 and C851 are indicated and can bond in three different configurations: C792-C827, C827-C829 (blue spheres) and C829-C851.

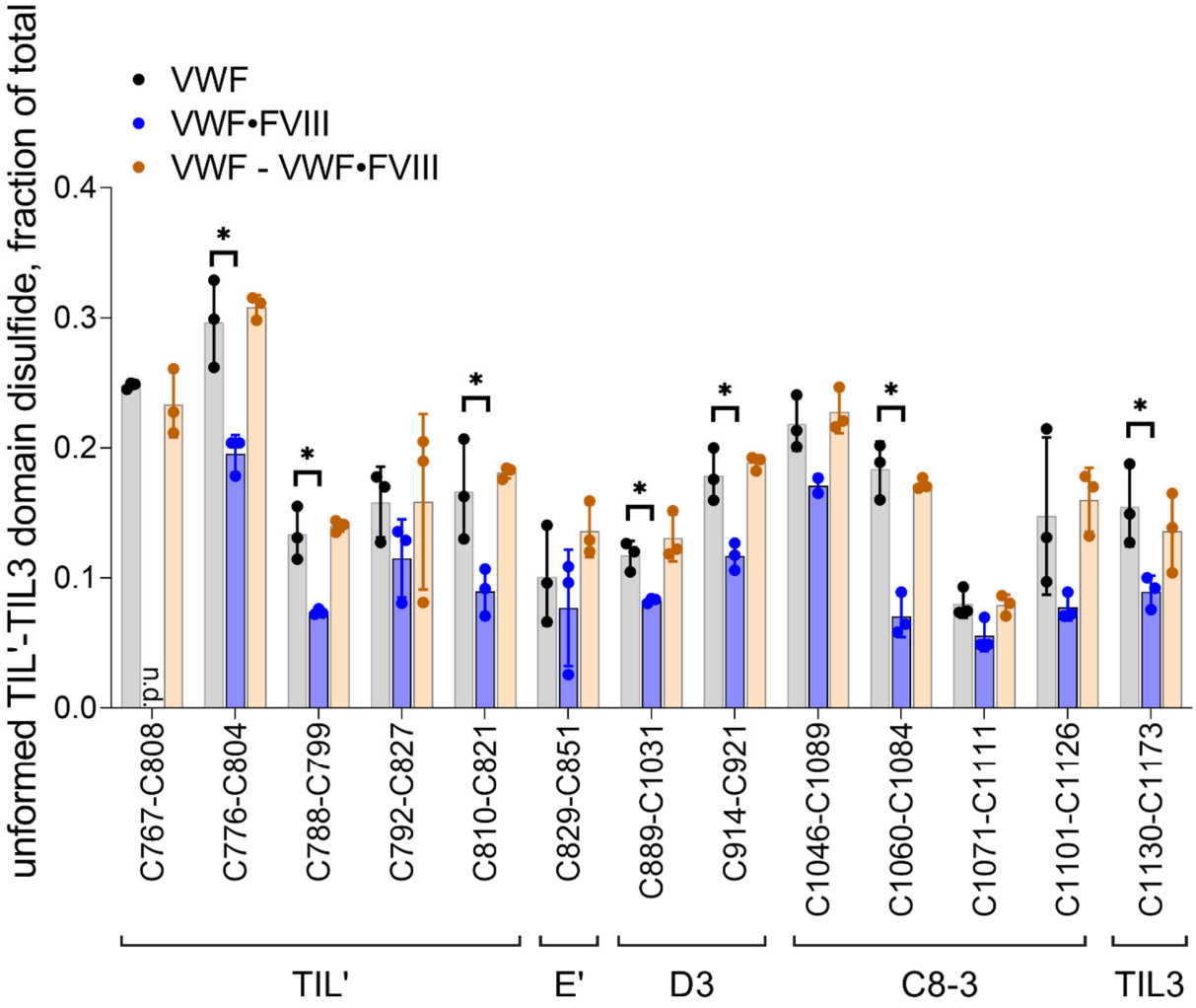

Figure S7. Binding of pegylated FVIII to VWF results in formation of VWF TIL'-TIL3 disulfides. Comparison of the redox states of the VWF TIL'-TIL3 disulfides in three healthy human donors (2 males, 1 female) (black symbols), the plasma VWF bound to pegylated human recombinant full-length FVIII (Adynovate, Takeda, blue symbols) and the unbound VWF in plasma following removal of VWF·FVIII complexes (orange symbols). The bars and errors are mean ± SD. Parametric unpaired t test was used to evaluate differences between groups. Significant difference ($p < 0.05$) between VWF and VWF·FVIII groups is indicated by *. There was no significant difference between the VWF and VWF - VWF·FVIII groups. Peptides that were not resolved in the experiment are indicated as not determined (n.d.).

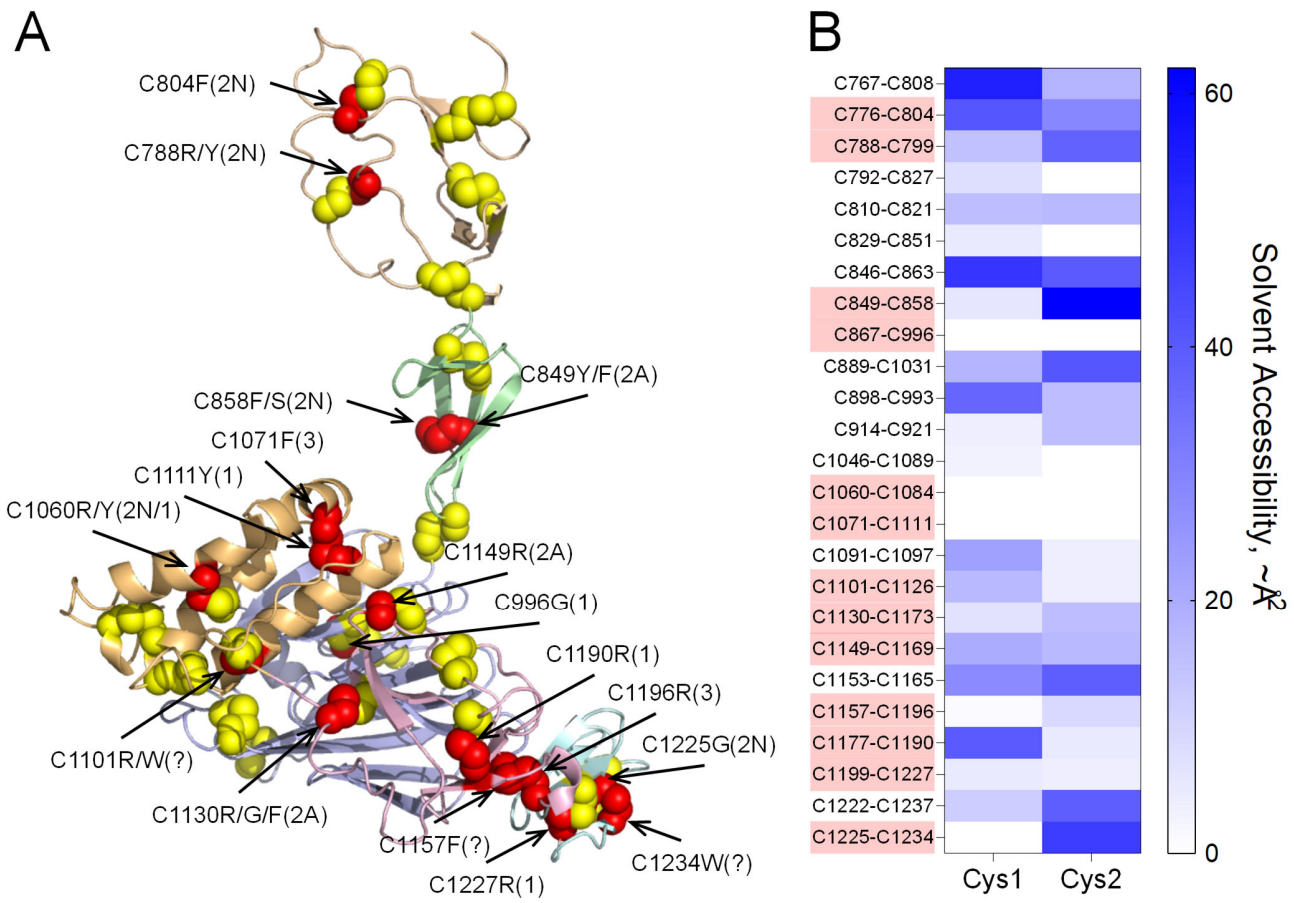

Figure S8. VWD mutations in disulfide bond cysteines at the FVIII binding site. **A**. Ribbon representation of the crystal structure of the TIL' (residues 764-827 in wheat), E' (residues 828-863 in light green), D3 (residues 864-1037 in light blue), C8-3 (residues 1038-1127 in light orange), TIL3 (residues 1128-1196 in pink) and E3 (residues 1197-1252 in cyan) domains of VWF [2] (PDB identifier 6n29). The cysteine residues comprising the 25 disulfide bonds are shown as spheres. Red spheres indicate VWD cysteine mutations that have been identified in patients. The cysteine residue mutation and VWD type is indicated. Mutations listed in the EAHAD von Willebrand Factor Variant Database as of December 20, 2020 are indicated. The C788R/Y, C804F, C858F/S C1060R/Y and C1225G mutations result in impaired binding of FVIII but not production of VWF, or type 2N VWD. Both the C788R and C1225G mutations have been shown to be type 2N mutations with both reduced secretion and multimerization. Thus, these mutations likely impair protein folding and/or exit from the ER. **B**. Heat map of the solvent accessibility of the 50 VWF disulfide bond cysteines in the TIL'-TIL3 domains. The scale is the solvent accessibility in ~Å^2 derived from DSSP [3] using the PDB identifier 6n29 structure [2]. The TIL'-TIL3 structure crystallized as a dimer and to avoid possible masking of surface exposed cysteines at the dimer interface, chain A of the structure was extracted and analyzed independently. The disulfides highlighted in red are those mutated in VWD and shown in part A.

References

1. Obeidy P, Wang H, Du M, et al. Molecular Spring Constant Analysis by Biomembrane Force Probe Spectroscopy. *J Vis Exp*. 2021(177).
2. Dong X, Leksa NC, Chhabra ES, et al. The von Willebrand factor D'D3 assembly and structural principles for factor VIII binding and concatemer biogenesis. *Blood*. 2019;133(14):1523-1533.
3. Kabsch W, Sander C. Dictionary of protein secondary structure: pattern recognition of hydrogen-bonded and geometrical features. *Biopolymers*. 1983;22(12):2577-2637.